ZIGBEE PROTOCOL AND MICROCONTROLLER ON A PV SYSTEM FOR A MILKING CATTLE ROBOT

Tomáš TESAŘ[1], Petr VACULÍK[1], Rui MELICIO[2], Victor M.F. MENDES[3]

[1]*Department of Technological Equipment of Buildings, Czech University of Life Sciences Prague*
[2]*ICT, Departamento de Física, Escola de Ciências e Tecnologia, Universidade de Évora, Portugal*
[3]*CISE, Electromechatronic Systems Research Centre, Universidade da Beira Interior, Portugal*

Abstract
This paper is about a system for supporting action of management in an industrial building integrated photovoltaic system by a supervising and monitoring data collector system of environmental data. The integrated photovoltaic system is a grid-connected rooftop-mounted having energy storage with the main purpose of supplying energy for an industrial milking cattle robot. The main equipment of the robot, the photovoltaic system is summarized and the equipment for supporting the assessment of the environmental data is further addressed. This equipment play an important role in nowadays for industrial milking and even more important in a smart grid context. Sensors, actuators and ZigBee technology are used in an association with Arduino allowing to have available information to carry way the management. Finally, conclusions are addressed about the hardware for the supervising and monitoring.

Key words: *PV system; milking cattle robot; monitoring; wireless sensors; microcontroller; ZigBee.*

INTRODUCTION

The study in this paper is about a Building Integrated PV (BIPV) roofing system with a wireless monitoring and control based on the ZigBee protocol. As main downstream devices, the roofing system accommodates power for a milking cattle robot and an energy storage intended to partially or fully side-step the supplying of energy from the electric utility. The system under study can enable further functionality, for instance, can enable control of sun radiance and temperature in rooms, protection or safety control of the building. The International Energy Agency Implement of Photovoltaic Power Systems Operational Performance of PV Systems and Subsystems (IEA PVPS Task 2) has established a set of parameters describing the operational performance of PV systems in buildings (*Batista et al., 2014; Boonmee et al., 2009*). The main parameters associated with the performance are: module temperatures, solar irradiation, wind speed, the DC power generated by the PV system, the AC grid voltage, and the AC current injected into the grid (*Batista et al., 2014; Boonmee et al., 2009*). The ZigBee technology has been gathering great acceptance (*Fadlullah et al., 2011*), advantaging from having low power consumption, low cost and an outstanding wireless networking protocol to be used in wireless connections in automation and remote-control (*Batista et al., 2014*). The IEEE 802.15.4 is a standard for a Low-Rate Wireless Personal Area Network (LR-WPAN) defining the Physical Layer (PHY) and Media Access Control (MAC) and is maintained by the IEEE 802.15 working group (*Batista et al., 2014*). LR-WPAN supports low cost modules, low power consumption, secure communication, data collision avoidance and power management (*Batista et al., 2012a; Batista et al., 2012b*). The ZigBee technology is a specification based on the IEEE 802.15.4 standard extending that definition by developing extra new higher layers. ZigBee technology can be implemented in mesh networks, with a larger range, than the Bluetooth technology. This technology is expected to transmit from 1 m to 100 m, depending of the in-situ environment sources of interference and of the power output consumption (*Batista et al., 2012*a). The IEEE 802.15.4 standard defines two different types of devices: Full Function Devices (FFD) or Reduced Function Devices (RFD). An FFD can communicate with any other device and perform all the functions defined on the standard, including relaying messages and sensor/actuator tasks. An FFD can play the role of coordinator, router or end device in the Personal Area Network (PAN) powered from an AC supply to be always active and monitoring the PAN (*Batista et al., 2012b*). An RFD requires relatively small resources memory size, compatible with a lower processing capability and allowing a decrease on the final cost. Typically, an RFD must be connected to an FFD and are not used to act as a coordinator or as a router but as an end device such as a sensor or an actuator performing limited tasks (*Batista et al., 2012b*). There are two types in IEEE 802.15.4 for the topology: Peer to Peer or Star. The Peer to Peer topology as shown allows the creation of Cluster-tree networks. This topology also as shown allows the creation of mesh networks, allowing all messages to be routed to any other FFD. In the Star topology the FFD acting as a coordinator is the central node having other FFD and RFD nodes attached directly to the coordinator (*Batista et al., 2012a; Batista et al., 2012b*). ZigBee technology has a wide acceptance and successful operates in many applications (*Batista et al., 2012b*). A wireless sensor network is valuable technology for monitoring a PV system using radio frequency transceivers, sensors and microcontrollers. Wireless sensor networks have embedded self-organizing, self-configuring, self-diagnosing and self-healing capability. The aim of this study about a BIPV real implementation with a remote monitoring data system for the PV system having a storage battery, supplying power to a milking cattle robot, situated in Žďár nad Sázavou, Czech Republic. The main parameters collected on in situ are: solar irradiance, wind speed and temperature. Prototypes of sensors for temperature, pyranometer and one anemometer are performed using microcontroller Arduino hardware and software and the ZigBee network technology interfaces the system with a Python software. The rest of the paper is organized as follows. Section II presents the main framework the followed procedure a summarizes the robot and the PV systems. Section III presents the Monitoring Data Collector. Finally, concluding remarks are in Section IV.

MATERIALS AND METHODS

The sensor prototypes implemented for the tests are: a ZigBee coordinator module with processing capability offered by an Arduino board as in (*Batista et al., 2014*; *Georgitzikis et al., 2012*); a ZigBee end-nodes connected to the Arduino board; and a ZigBee module that will function only as router. The ZigBee end-node in the receiver side is also attached to an Arduino board that reads the Received Signal Strength Indicator (RSSI) and displays the value in an LCD screen in decibel-milliwatts [*dBm*]. The field tests test the RSSI information and the loss of data. The ZigBee communication devices are configured to operate in an Application Programming Interface (API) mode, delivering the RSSI information of a module. This module receives the message and the checksum byte of the packets data frame validating if the data arrives without errors (*Batista et al., 2014*). The relation between transmitted power and the received power is given by the Friis transmission equation (*Batista et al., 2014*) given by:

$$\frac{P_r}{P_t} = G_t . G_r . \left(\frac{\varphi}{4.\pi.d}\right)^2 \tag{1}$$

In (1) where P_t and P_r are respectively the transmitted power and the received power which has to be higher than the sensitive of the receiver, P_t and P_r are in the same units of power; G_t and G_r are respectively the gains of the transmitter and the receiver antennas; φ is the wavelength given by the channel in the ZigBee devices; d is the distance between the transmitter and the receiver antennas. φ and d are in the same units of length. The received signal strength indicator final $\overline{RSSI}$ value is taken in the ZigBee (*Batista et al., 2014*). The signal strength is given by:

$$\overline{RSSI} = \frac{1}{n}\sum_{i=1}^{n} RSSI_i \tag{2}$$

In (2) n is the number of samples. The RSSI value only reflects the received signal strength of the last message hop and not the signal strength of all the routers (multihops), neither the general quality of the transmission. So, if a device is connected to a router, the RSSI value only represents the signal strength between the last router and the device and not between the ZigBee coordinator sending the message and the device (*Batista et al., 2014*). Before the sensor modules installation, an evaluation of the ZigBee devices location is made by evaluating the RSSI value for different positions. At the transmitter side the Arduino board with the ZigBee coordinator operating in API mode is configured to send data packets to a predefined ZigBee device under analysis for the RSSI signal analysis, which has a predetermined 64 bit network address. These packets are sent in intervals of 5 s. At the receiver side the ZigBee end-node has a microcontroller Arduino board that reads the RSSI value by taking n samples in intervals of 5 s and then averaging the samples to be displayed. Concerns with the installation of sensors, for instance, information to be delivered to the destination, insurance of delivering without errors or faults (*Batista et al., 2017*) have been taken into consideration. The data collector is a support information system for the schedule of needed energy considering the capture by BIPV roof system and the stored energy, having the main purpose of supplying power to a milking cattle robot situated in a farm in Žďár nad Sázavou, Czech Republic. The objective is avoiding as much as possible the usage of electric energy from the electric grid utility. The farm has around 70 cows to be milked and installed the milking cattle robot in 2008. The milking cattle robot is one of the first milking cattle robots installed in the Czech Republic by the company DeLaval. The Robot installed is a single-blade milking robot having two parts. The first part consists of a cage box in the form of a container and is made of stainless-steel resistant to corrosion. The box is very spacious, the teat cups can be deployed in the teats of the cow by human intervention. The entrance and exit doors are electronically controlled to be opened and closed by a hydraulic motor. The doors positioning is on the side of the box and the dairy cows pass through the arc when passing through the milking robot. There is an identification set on the box structure. The floor is a non-slip rubber with built-in nozzles to easily clean the dirt from a hygienic point of view. The second part of the milking robot is the engine room where the hydraulic two-articulated rotary milking arm of the stainless steel is located. The milking arm performs the test preparation before milking, the teat cup deployment and re-deployment. If necessary, then a correction is made for the position of the milk hose and teats disinfection after milking. This arm is inspired in the human hand and easily responds to the tear irregularities with a deflection of up to 45° in a wide range, of high or low seated of mammary gland of the cows. There is on the shoulder an optical camera and a double laser. There are four teat cups hanging beside their shoulders able to drip and remain free of dirt, and the fifth handpiece cleaning the udder is placed under the same principle as the teat cups of the quarter. The robot is equipped with an oil-free air compressor and four optical milk counters for each area to monitor deviations and abnormalities in flow, bed, admixture and blood flow rates. The Robot LCD displays information coming from the software processing decision making and recording event and data. The energy for the Robot is supplied by the: PV system, 15 battery system installed in the farm or the local electric grid. The PV array has a power of 5.25 kWp and is composed by 21 PV panels of Polycrystalline technology Omsun 250 W with an allowed module operating temperature of -40 to 85 ºC and the Normal Operating Cell Temperature (NOTC) is 45±2 ºC. More data at standard test conditions (STC) for the modules Omsun 250 W (*Omsun, 2019*) are shown in Tab. 1.

Tab. 1 STC DATA OF OMSUN 250 W

Technology	V_{MP}	I_{MP}	V_{OC}	I_{SC}	*Efficiency*
Polycrystalline	31.36 V	7.98 A	38.41 V	8.51 A	15.20 %

In Tab. 1 the values for the voltage and current at maximum power give a power of 250 Wp per PV module and a form factor of 76 % at STC, but due to ageing a value of 0.60 %/year of degradation is to be expected. The balance-of-system has a battery management system as usually included in the DC circuit and the power inverter implemented has anti-islanding protection. The inverter is compatible with the PV systems power and with the three-phase bus bar of the AC circuit connecting to the electric grid utility. The inverter implemented is a three-phase PV power inverter GoodWe GW10K-DT. The sensors and the data transmitter are installed near the PV arrays on the roof of one of the buildings. While the receiver and monitoring data collector are installed in another, see Fig. 1 a). The PV array and the monitoring by the sensors of wind speed, irradiance and temperature in situ are near of the PV arrays as shown for the pyranometer and the anemometer respectively in Fig. 1 a), b), c), d). In Fig. 1 b) the cup anemometer shown has a range between 0.9 m/s and 40 m/s and the electrical output has a frequency of 100 Hz for a wind speed of 40 m/s. This anemometer, 4.3515.51.105 is produced by (*Thies Clima, 2019)*. In Fig. 1 c) the pyranometer shown has the spectral range between 310 nm and 2800 nm, the time response is less than 18 s. Although this time is greater than the response of the PV modules, this difference is not relevant for the purpose of monitoring PV modules (*Boonmee et al., 2009*). This pyranometer, CM6B (*Thies Clima, 2019*), is produced by Kipp and Zonenand is based on a thermocouple device. In Fig. 1 d) the temperature sensor shown is a digital thermometer, DS18B20, produced by Maxim Integrated (*Maxim Integrated, 2019*), providing 9 bit to 12 bit Celsius measurements in a range between -55 ºC and +125 ºC and has an alarm function with non-volatile user programmable upper and lower trigger points.

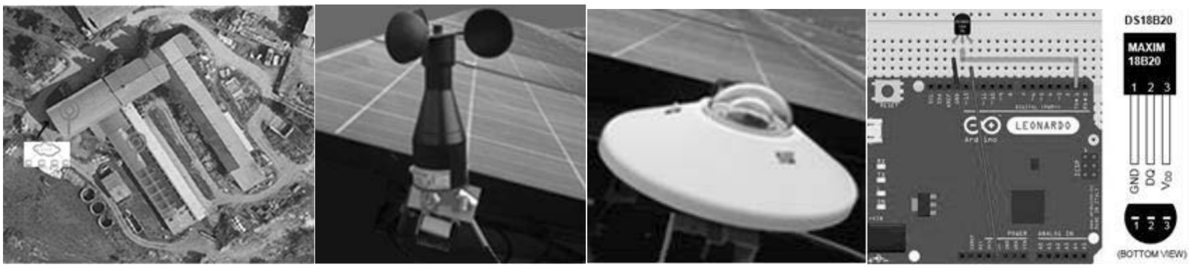

a) b) c) d)

Fig. 1 Sensors: a) PV array, b) anemometer, c) pyranometer, d) temperature sensor and Arduino.

RESULTS AND DISCUSSION

The distance between the transmitter antenna near the PV arrays and the receiving antenna at the building where the monitoring data collector is located is about 40 m and the wireless transmission shown in Fig. 1 a) is implemented by ZigBee network technology. Normally, a linear increase on the maximum power is expected with the increase in the irradiance. Also, the power output of a PV cell can be considered as an affine function of the PV cell temperature (*Woyte et al. 2013*): a reduction on power for the OMSUN 250 W of 0.475 % is expected per 1ºC of increase in the PV module. The energy capture by the PV arrays for one day depends on the in situ peak sun-hours, which is the in situ irradiation per unit of area in $[kWh/m^2]$ computed by the integral of the irradiance over the time. So, the parameters influencing the capturing of energy by the PV system in situ are: the horizontal component of the wind speed, the irradiance, the temperature where the PV modules are implemented. The cup anemometer produced by Thies Clima, 4.3515.51.105 (*Thies Clima, 2019*), measures the value of the angular frequency of the anemometer which is considered as an affine function of the wind speed. So, the anemometer transfer function (*Pindado el at., 2012)* is given by:

$$V = A.f + B \tag{3}$$

In (3) V is the wind speed [*m/s*], f is the output frequency [*Hz*], A and B are coefficients of the transfer function, the slope and the offset of the anemometer, respectively. The coefficients of the transfer function are established by a calibration process that correlates the wind speed and the output frequency. The global irradiance (*Thies Clima, 2019*) measured by a pyranometer is given by:

$$E_{\downarrow Solar} = \frac{U_{emf}}{S_{ensivity}} \tag{4}$$

In (4) $E_{\downarrow Solar}$ is the global irradiance in $[W/m^2]$, U_{emf} is voltage at the thermocouple in response of the subjected global irradiance in $[\mu V]$ and $S_{ensivity}$ is the sensitivity of the pyranometer in $[\mu V m^2/W]$. The calibration of the pyranometer is performed in accordance with ISO 9846 ISO 9847 (*Boonmee et al., 2009*; *Kipp and Zonen, 2019*), i.e., under indoor and outdoor conditions. The temperature sensor used is the digital thermometer produced by Maxim Integrated, DS18B20, (*Maxim Integrated, 2019*). The DS18B20 connected to the Arduino shown in Fig. 1 d) provides 9 bit to 12 bit Celsius measurements in a range between -55 ºC and +125 ºC and has an alarm function with non-volatile user programmable upper and lower trigger points. The supervising and monitoring data collector system of environmental data is equipped with a computer having a program in Python for recording and processing the collected data. The network node with the Arduino, the transmitting ZigBee and the prototype sensors is interfaced with the other equipment as shown in Fig. 2.

a) b) c)

Fig. 2 a) Network node with the sensors, Arduino and ZigBee data transmitter; b) AC/DC onsite installation; c) Node with ZigBee data receiver and computer for recording and processing data.

In Fig. 2 a) the network node shown is for collecting and transmission of data, the input information from the anemometer 4.3515.51.105, the pyranometer CM6B and temperature sensor DS18B20 is sent to the Arduino and there is a bidirectional flow of information between the Arduino and the ZigBee. In Fig. 2 b) the power AC/DC installation is shown under the roof of the building where the PV modulus are installed. In Fig. 2 c) the network node shown is for receiving and processing the information: another bidirectional flow of information is implemented between the ZigBee and the Arduino and from the Arduino to a computer to be analyzed and process the data by a Python script. An instance of historical data for the wind speed, the irradiance and temperature collected during a day are respectively shown in Fig. 3 a), Fig. 3 b) and Fig. 3 c).

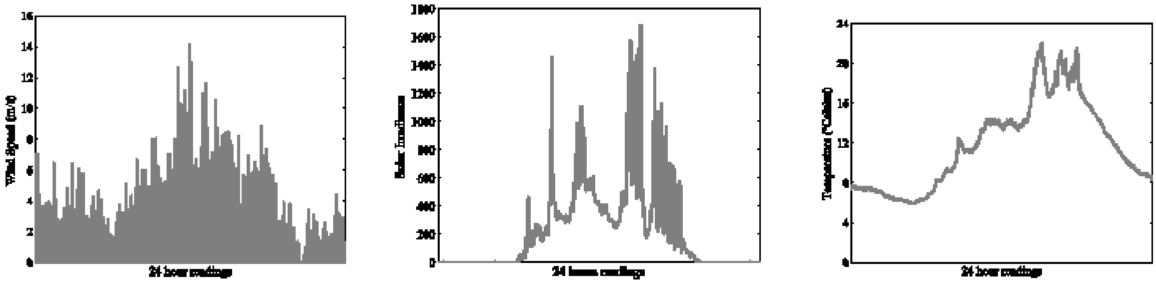

a) b) c)

Fig. 3 Data collected in a day: a) wind speed, b) solar irradiance, c) ambient temperature.

In Fig. 3 the wind speed, solar irradiance and ambient temperature data shown can to use as an instance of historical data to predict the power and energy captured by the PV system, considering the NOCT (*Omsun, 2019*), the ambient temperature, the irradiance and the temperature of the PV cell can be computed. Also, $P_{MP} = V_{MP} \times I_{MP}, V_{OC}$ and I_{SC} can be computed using the temperature coefficients (*Omsun, 2019*), the change on the irradiance relatively to the one Sun irradiance, i.e., STC irradiance of 1 kW/m^2, and the wind speed: an increase on the wind speed extracts more thermal energy from the modules, implying that the temperature of the module decreases.

CONCLUSIONS

The BIPV system with the PV system installed on the roof of the Žďár nad Sázavou, Czech Republic, is an instance of a grid-connected rooftop-mounted system aiming at a sustainable EU industrial milking by a milking cattle robot. This BIPV systems reduces or off-sets the usage of electric energy from the grid of the electric utility. Further, as the BIPV has storage and PV energy, the industrial milking has electric power without too much concern about the continuity of energy supply from the utility. So, the stored and PV energy avoids stopping the operation of the milking cattle robot with a jumpy cow stuck inside of the robot due to an eventual discontinuity of energy supply from the utility. But needs a convenient system for supporting the action of management in the BIPV and a part of that systems is a supervising and monitoring data collector of environmental data. The monitoring data collector for the PV system installed is hardware and software to collect, send and process the values of wind speed, irradiance and temperature in the environment where PV modules are located. The monitoring is addressed for the data collector collecting data from the sensors of wind speed, irradiance and temperature in order to be processed to deliver information on the operation condition of the PV modules. The development of prototypes of sensors using low power wireless networks is based on the Arduino microcontroller hardware and ZigBee protocol. The ZigBee standard proved to be a reliable approach for the creation of wireless network for monitoring at a reasonable cost.

ACKNOWLEDGMENT

The first author would like to thank the ERASMUS+ Erasmus Mundus project for funding the scholarship. This work is funded by Funds through the European Union through the European Regional Development Fund, included in the COMPETE 2020 (Operational Program Competitiveness and Internationalization) through the ICT project (UID/GEO/04683/2019) with the reference POCI010145FEDER007690; Portuguese Funds through the Foundation for Science and Technology-FCT under the project LAETA 2015- 2020, reference UID/EMS/50022/2019; Portuguese Foundation for Science and Technology (FCT) under Project UID/EEA/04131/2019.

REFERENCES

1. Batista, N.C, Melício, R., & Mendes, V.M.F. (2014). Layered smart grid architecture approach and field tests by ZigBee technology. *Energy Conversion and Management, 88*, 49-59.
3. Batista, N.C., Melício, R., Matias, J.C.O., & Catalão, J.P.S. (2012a). ZigBee devices for distributed generation management: field tests and installation approaches. In *Proc. of the 6th IET International Conference on Power Electronics, Machines and Drives - PEMD 2012* (pp. 1-5). Bristol, UK.
4. Batista, N.C., Melício, R., Matias, J.C.O., & Catalão, J.P.S. (2012b). ZigBee standard in the creation of wireless networks for advanced metering infrastructures. In *Proc. of 16th IEEE Mediterranean Electrotechnical Conference* (pp. 220-223). Yasmine Hammamet, Tunisia.
5. Boonmee, C., Plangklang, B., & Watjanatepin, N. (2009). System performance of a three-phase PV-grid-connected system installed in Thailand: data monitored analysis. *Renewable Energy, 34*, 384-389.
6. Fadlullah, Z.M., Fouda, M.M., Kato, N., Takeuchi, A., Iwasaki, N., & Nozaki, Y. (2011). Toward intelligent machine-to-machine communications in smart grid. *IEEE Communications Magazine, 49*, 60-65.
2. Batista, N.C., Melício, R., & Mendes, V.M.F. (2017). Services enabler architecture for smart grid and smart living services providers under industry 4.0. *Energy and Buildings, 141*, 16-27.
7. Georgitzikis, V., Akribopoulos, O., & Chatzigiannakis, I. (2012). Controlling physical objects via the internet using the Arduino platform over 802.15.4 networks. *IEEE Latin America Transactions, 10,* 1686-1689.
8. Kipp & Zonen. (2019). Retrieved from http://www.kippzonen.com/Product/12/CMP-6-Pyranometer#.VUaeePlVhBc.
9. Maxim Integrated. (2019). Retrieved from http://www.maximintegrated.com/.
10. Omsun. (2019). Retrieved from http://www.kazan-haz.hu/files/napelem/omsun-250w-poly.pdf
11. Pindado, S., Sanz, A., & Wery, A. (2012). Deviation of cup and propeller anemometer calibration results with air density. *Energies, 5*, 683-701.
12. Thies Clima (2019). Retrieved from http://www.thiesclima.com/.
13. Woyte, A., Richter, M., Moser, D., Mau, S., Reich, N., & Jahn, U. (2013). Monitoring of photovoltaic systems: good practices and systematic analysis. In *Proc. of 28th European Photovoltaic Solar Energy Conference and Exhibition – PVSEC (*pp. 1-9). Paris, France.

Corresponding author:
Ing. Tomáš Tesař, Department of Mechanical Engineering, Faculty of Engineering, Czech University of Life Sciences Prague, Kamýcká 129, Praha 6, Prague, 16521, Czech Republic, phone: +420 22438 3178, e-mail: tesart@tf.czu.cz